

Learning from Good and Bad Decisions: A Data-driven Inverse Optimization Approach

Houra Mahmoudzadeh

Department of Management Sciences, University of Waterloo, ON, Canada. houra.mahmoudzadeh@uwaterloo.ca

Kimia Ghobadi

Malone Center for Engineering in Healthcare, Center for Systems Science and Engineering, Department of Civil and Systems Engineering, Johns Hopkins University, Baltimore, MD, USA. kimia@jhu.edu

Conventional inverse optimization inputs a solution and finds the parameters of an optimization model that render a given solution optimal. The literature mostly focuses on inferring the objective function in linear problems when acceptable solutions are provided as input. In this paper, we propose an inverse optimization model that inputs several accepted and rejected solutions and recovers the underlying convex optimization model that correctly classifies these given solutions. The novelty of our model is three-fold: First, while most literature focuses on inferring the objective function only, we focus on inferring the feasible region. Second, our model is capable of inferring the constraints of general convex optimization models. Third, the proposed model learns from both accepted (good) and rejected (bad) observations in inferring the constraint set. The resulting model is a mixed-integer nonlinear problem, and to mitigate its complexity, we use the theoretical properties of its solutions to derive a reduced reformulation that is easier to solve. Using a case study on radiotherapy treatment planning for breast cancer patients, we demonstrate that our proposed model can infer a set of clinical guidelines to classify accepted and rejected plans with over 95% accuracy.

Key words: inverse optimization, constraint inference, model learning, convex optimization, radiation therapy.

1. Introduction

In the era of big data, learning from past decisions and their corresponding outcomes, whether good or bad, provides an invaluable opportunity for improving future decision-making processes. While there is considerable momentum to learn from data through artificial intelligence, machine learning, and statistics, the field of operations research has not been using this valuable resource to its full

potential in learning from past decisions to inform future decision-making processes. One of the emerging methodologies that can benefit from this abundance of data is inverse optimization (Ahuja and Orlin 2001).

A regular (forward) optimization problem models a system and determines an optimal solution that represents a decision for the system. On the contrary, inverse optimization aims to recover the optimization model that made a set of given observed solutions (or decisions) optimal. For instance, in radiation therapy treatment planning for cancer patients, radiation oncologists make decisions on whether the quality of personalized plans generated through a treatment planning system is acceptable for each patient. In this case, an inverse model would be able to learn the implicit logic behind the oncologist's decision-making process. Traditionally, the input to inverse models almost exclusively constitutes optimal or near-optimal solutions, and little attention has been paid to learning from unfavorable solutions that must be avoided. In inverse optimization, learning from both 'good' and 'bad' decisions can provide invaluable information about the patterns, preferences, and restrictions of the underlying forward optimization model.

Inverse optimization is well-studied for inferring linear optimization models (Chan et al. 2021). This focus is mostly due to the tractability and existence of optimality guarantees in linear programming. In practice, however, nonlinear models are sometimes better suited for characterizing complex systems and capturing past solutions' attributes. The literature also largely focuses on inferring the utility function of decision-makers, which can be interpreted as the objective function of an optimization problem when the feasible region is known. Inferring the feasible region itself, on the contrary, has not received much attention, which may be attributed to the fact that inverse models for constraint inference are nonlinear, even when the forward problem is linear. For linear problems, there have been recent attempts for recovering the forward feasible region through inverse optimization (Chan and Kaw 2020, Ghobadi and Mahmoudzadeh 2021), however, these studies do not generalize to nonlinear problems and do not incorporate bad decisions in constraint inference.

In radiation therapy treatment planning for cancer patients, a large pool of historical treatment plans exists that can be used in an inverse learning process. A plan is often designed to meet a set of pre-determined and often conflicting constraints, which are referred to as clinical guidelines. These guidelines are blanket statements and not personalized, which means they may be too strict or too relaxed (sometimes simultaneously) for individual patients. As a result, some plans that satisfy the original guidelines may be rejected and some seemingly infeasible plans may be accepted. This application lends itself well to using inverse optimization for inferring the true underlying clinical guidelines for patient populations, which can lead to more efficient treatment planning and improved quality of treatment. While much attention has been paid to understanding the tradeoff balance in the objective of cancer treatment using inverse optimization, the problem of understanding and constructing proper clinical guidelines remains under-explored. An incorrect guideline or constraint in the optimization model can lead to a significantly different feasible region and affect the possible optimal solutions that the objective function can achieve.

In this paper, we focus on recovering the constraints of an optimization model through a novel inverse optimization model for general convex optimization problems. Our model inputs a set of past expert solutions, both accepted (good) and rejected (bad), and uses it to infer the underlying optimization problem that makes these past decisions feasible or infeasible, respectively. We further propose a reduced reformulation of our inverse optimization model to mitigate its complexity and improve solvability. We demonstrate the merit of our framework using the problem of radiation therapy treatment planning for breast cancer patients where we impute the underlying conditions that correctly characterize acceptable and non-acceptable treatment plans.

1.1. Literature Review

Given a (forward) optimization problem with a set of partially known parameters, inverse optimization inputs a set of given solution(s) and recovers the full set of parameters (Ahuja and Orlin 2001). The input solution is often a single observation that is optimal (Ghate 2020b, Iyengar and Kang 2005) or near-optimal (Aswani et al. 2018, Bertsimas et al. 2015, Chan et al. 2019, 2014b,

Keshavarz et al. 2011, Naghavi et al. 2019) in which case the inverse model minimizes a measure of the optimality gap. Recently, with more focus on data-driven models, multiple observations have also been considered as the input to inverse models (Babier et al. 2021, Bertsimas et al. 2015, Chow and Recker 2012, Esfahani et al. 2018, Keshavarz et al. 2011, Troutt et al. 2008, 2006, Zhang and Liu 1999). Since not all of the input observations can be (near-)optimal, a measure of the collective data is often optimized instead. Some studies also consider noise or uncertainty in data that affect the inverse models (Aswani et al. 2018, Dong and Zeng 2018, Ghobadi et al. 2018), or infer the structure of solutions to the inverse model instead of reporting a single inverse solution (Tavashioğlu et al. 2018). For a comprehensive review of inverse optimization, we refer the readers to the review paper by Chan et al. (2021).

Inverse optimization has found a wide range of applications including energy (Birge et al. 2017, Brucker and Shakhlevich 2009), dietary recommendations (Ghobadi et al. 2018), finance (Li 2021), and healthcare systems (Chan et al. 2022), to name a few. In particular, radiation therapy treatment planning for cancer has been studied in the context of inverse optimization (Ajayi et al. 2022, Babier et al. 2018, 2020, Boutilier et al. 2015, Chan et al. 2022, Chan and Lee 2018, Chan et al. 2014b, Ghate 2020a, Goli et al. 2018, Lee et al. 2013). The current literature mostly focuses on recovering the objective function and better understanding the underlying complex tradeoffs between different objective terms in the radiation therapy treatment plans. For instance, both Chan and Lee (2018) and Sayre and Ruan (2014) input accepted treatment plans to recover the appropriate weights for a given set of convex objectives using inverse optimization. Gebken and Peitz (2021) finds the objective weights for unconstrained problems using singular value decomposition. Personalization for different patient groups has been explored by Boutilier et al. (2015) by recovering the utility functions appropriate to each group. Ajayi et al. (2022) employs inverse optimization for feature selection to identify a sparse set of clinical objectives for prostate cancer patients. These studies exclusively used accepted treatment plans as an input to the inverse models. When the accepted plans are infeasible with respect to guidelines, the inverse models aim to infer the forward objective that makes them near optimal.

The current inverse optimization literature mainly focuses on inferring the objective function of the underlying forward problem (Chan et al. 2021). Constraint inference, on the contrary, has received little attention. Recovering the right-hand side of the constraint parameters alongside the objective parameters has been explored by Chow and Recker (2012), Dempe and Lohse (2006) and Černý and Hladík (2016). Similarly, Birge et al. (2017) recover the right-hand side parameters so that a given observation becomes optimal utilizing properties of the specific application and Dempe and Lohse (2006), Güler and Hamacher (2010), Saez-Gallego and Morales (2018) make a given observation (near-)optimal. Chan and Kaw (2020) perturb the nearest facet to make a given observation optimal and hence, find the left-hand side parameter of a linear constraint when the right-hand side parameters are known. Closest to our work is the study by Ghobadi and Mahmoudzadeh (2021) when the full set of the constraint parameters is unknown in a linear model but the objective function and a set of feasible observations are given. Their method utilizes linear properties of the forward optimization and does not generalize to convex forward problems.

Inverse optimization has been extensively considered for inferring linear optimization models. However, the underlying forward optimization is assumed to be nonlinear, and sufficient conditions for optimality of observations cannot be guaranteed unless the model falls under specific classes such as convex or conic optimization for which Karush-Kuhn-Tucker (KKT) conditions are sufficient for optimality (Boyd and Vandenberghe 2004). Keshavarz et al. (2011) consider general convex models and use past observations to recover the objective function parameters by minimizing the optimality errors in KKT conditions. Aswani et al. (2019) explore nonlinear convex optimization to recover the objective function when the data is noisy. Zhang and Xu (2010) recover the objective function for linearly-constrained convex separable models. In another paper, Zhang and Zhang (2010) propose an inverse conic model that infers quadratic constraints and shows that it be efficiently solved using the dual of the obtained semi-definite programs. While these studies have advanced the theory of inverse optimization for inferring nonlinear forward models, the focus has been the inference of the utility function of decision-makers, which translates to inferring the objective function of the forward models, and constraint inference has not received much attention in the literature.

Most importantly, inverse models have traditionally focused on learning from ‘good’ decisions only, which are typically feasible for the forward problem. The inclusion of infeasible observations has been explored by [Ahmadi et al. \(2020\)](#), [Babier et al. \(2021\)](#), [Chan et al. \(2022\)](#), [Shahmoradi and Lee \(2021\)](#), among others, when inferring the objective function parameters. However, because the feasible region is pre-determined in these studies, any infeasible observation is still treated as a ‘good’ decision that needs to be made near-optimal for the inferred objective. Hence, infeasible and feasible observations are used in a similar manner in order to extract information about the utility function and provide objective parameter trade-offs in the forward problem. When imputing constraint parameters, on the contrary, infeasible observations can be treated as ‘bad’ decisions. Hence, they can provide an additional layer of information by enabling a better determination of where the feasible region should reside, which areas should be excluded from it, and which constraint parameters would provide a better fit. To our knowledge, there has been no work that uses both feasible and infeasible observations in inferring the constraints of a linear or general convex forward problem.

1.2. Cancer Treatment Motivation

In 2022, there will be an estimated 1.9 million new cancer cases diagnosed and 609,360 cancer deaths in the United States, and approximately 60% of them will receive radiation therapy as part of their treatment ([American Cancer Society 2022](#)). The radiation therapy treatment planning process is a time-consuming process that often involves manual planning by a treatment planner and/or oncologist. The input of the planning process is a medical image (e.g., CT, MRI) which includes contours that delineate the cancerous region (i.e., tumor) and the surrounding healthy organs at risk (OAR). The goal is to find the direction, shape, and intensity of radiation beams such that a set of clinical metrics on the tumor and the surrounding healthy organs is satisfied. In current practice, there are clinical guidelines on these radiation metrics. However, these guidelines are not universally agreed upon and often differ per institution. Additionally, adherence to these guidelines is at the discretion of oncologists based on the specific needs of each patient.

Planners often try to find an acceptable treatment plan within these guidelines to forward to an oncologist who will, in turn, either approve or reject the plan. If the plan is not approved, the planner receives a set of instructions on which metrics to adjust to improve the plan. This iterative process can lead to unnecessary back and forth between the planner and the oncologist, may involve manual relaxation of criteria, and can result in suboptimal plans for patients. This process continues until the plan is approved.

There may exist approved treatment plans that do not meet all the clinical guidelines simultaneously, typically because there are trade-offs between different metrics, the guidelines are not personalized for each patient, and some radiation dose limits are too restrictive for some patients. Conversely, there may also exist plans that meet the guidelines but are not approved because the oncologist may find the guidelines too relaxed for some patients and believe better plans are achievable, which may also lead to an increased back and forth between the planner and the oncologist. In mathematical programming terminology, the implicit feasible region in treatment planning, based on which oncologists make an acceptance/rejection decision is unknown. A simplified schematic of accepted and rejected plans with respect to two metrics (Tumor dose and OAR dose) is shown in Figure 1(a). It can be seen that some points do not meet the guidelines but are accepted and others meet all guidelines but are rejected. The implicit constraints, however, always correctly classify the accepted/rejected plans.

In the radiation therapy treatment planning problem, we demonstrate that our inverse framework can learn from both accepted and rejected plans and infer the true underlying criteria based on which the accept/reject decisions are made. Finding such constraints enables us to better understand the implicit logic of oncologists in approving or rejecting treatment plans. In doing so, we help both oncologists and planners by (i) standardizing the guidelines and care practices, (ii) generating more realistic lower/upper bounds on the clinical metrics based on past observations, (iii) improving the quality of the initial plans according to the oncologist's opinion and hence, reducing the number of iterations between planners and oncologists, and (iv) improving the quality of

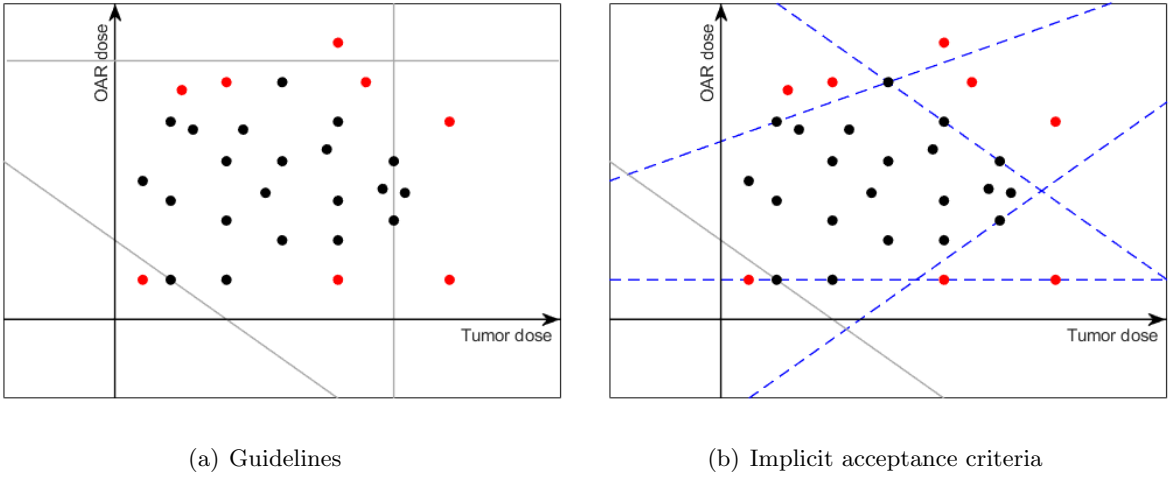


Figure 1 Simplified schematic representation of guidelines (gray solid) versus implicit (blue dashed) constraints. The black and red dots denote accepted and rejected plans, respectively.

the final plans by preventing low-quality solutions that otherwise satisfy the acceptability thresholds, especially for automated treatment planning methods that heavily rely on provided radiation thresholds and may result in infeasibility if clinical thresholds are not personalized.

2. Methodology

In this section, we first formulate a general convex forward optimization problem, where all or some of the constraints are unknown. We then define the inverse problem mathematically where a set of accepted and rejected observations are given, and the goal is to find constraint parameters that correctly classify these observations while enforcing optimality conditions on a preferred solution. We then present the general data-driven inverse optimization model and characterize the properties of its solutions.

2.1. Problem Definition

Let \mathcal{I} be the set of all constraints in a forward optimization problem. We denote the set of known nonlinear and linear constraints by \mathcal{N} and \mathcal{L} , respectively, and the set of unknown nonlinear and linear constraints to be inferred by $\tilde{\mathcal{N}}$ and $\tilde{\mathcal{L}}$, respectively. Note that $\mathcal{N} \cup \mathcal{L} \cup \tilde{\mathcal{N}} \cup \tilde{\mathcal{L}} = \mathcal{I}$ and $\mathcal{N}, \mathcal{L}, \tilde{\mathcal{N}}, \tilde{\mathcal{L}}$ are mutually exclusive sets. We note that the known constraints are a trusted subset of the guidelines that need to be satisfied by all future solutions, which can potentially be an empty

set. Assume that decision variable is $\mathbf{x} \in \mathbb{R}^m$. Let $f(\mathbf{x}; \mathbf{c})$ and $g_n(\mathbf{x}; \mathbf{q}_n)$, $\forall n \in \mathcal{N}$ be differentiable convex and concave functions on \mathbf{x} , respectively. The convex forward optimization (FO) model can be formulated as:

$$\text{FO :} \quad \underset{\mathbf{x}}{\text{minimize}} \quad f(\mathbf{x}; \mathbf{c}) \quad (1a)$$

$$\text{subject to} \quad g_n(\mathbf{x}; \mathbf{q}_n) \geq \mathbf{0}, \quad \forall n \in \mathcal{N} \cup \tilde{\mathcal{N}} \quad (1b)$$

$$\mathbf{a}'_\ell \mathbf{x} \geq b_\ell. \quad \forall \ell \in \mathcal{L} \cup \tilde{\mathcal{L}} \quad (1c)$$

Note that because $g_n(\mathbf{x}, \mathbf{q}_n)$ is concave, the constraint $g_n(\mathbf{x}; \mathbf{q}_n) \geq \mathbf{0}$ corresponds to a convex set. For brevity of notations, let the set of all known constraints be defined as $\mathcal{X} = \{\mathbf{x} \in \mathbb{R}^m \mid g_n(\mathbf{x}; \mathbf{q}_n) \geq \mathbf{0}, \forall n \in \mathcal{N}, \mathbf{a}'_\ell \mathbf{x} \geq b_\ell, \forall \ell \in \mathcal{L}\}$, the region identified by the known constraints of FO.

Assume that the structures of the functions $g_n(\mathbf{x}; \mathbf{q}_n)$, $\forall n \in \mathcal{N}$ are known, and the goal is to find unknown parameters \mathbf{q}_n , $\forall n \in \tilde{\mathcal{N}}$. Note $\mathbf{a}_\ell \in \mathbb{R}^m$ and $b_\ell \in \mathbb{R}$ are parameters of fixed size while each \mathbf{q}_n might be a vector of a different length $\mathbf{q}_n \in \mathbb{R}^{\phi_n}$, where ϕ_n depends on the type of nonlinear function that is to be inferred. For example, $g_1(\mathbf{x}; \mathbf{q}_1) = q_{11}x_1^2 + q_{12}x_2^2 + q_{13}x_1x_2 + q_{14}$ is a two-dimensional quadratic function with four unknown parameters q_{11}, \dots, q_{14} to be inferred. In what follows we describe the proposed inverse methodology for imputing the constraint parameters of the FO model.

2.2. Inverse Problem Formulation

Let \mathbf{x}_k , $k \in \mathcal{K}$ denote a set of given solutions corresponding to past decisions, where $\mathcal{K} = \mathcal{K}^+ \cup \mathcal{K}^-$ and \mathcal{K}^+ and \mathcal{K}^- denote accepted (good) and rejected (bad) observed decisions, respectively. In this section, we propose an inverse formulation that inputs these past decisions and infers the set of linear and nonlinear constraints of the forward problem such that all previously accepted constraints are inside the inferred forward feasible region and the rejected observations become infeasible. The inverse model also identifies a preferred solution based on the objective function of the forward problem and infers the forward feasible region such that this preferred point would be optimal for FO. Before introducing the inverse model, we first outline a few standard assumptions

on the structure of the problem and the observed data to ensure that the problem is well defined and feasible.

ASSUMPTION 1. *The functions $g_n(\mathbf{x}, \mathbf{q}_n)$ are well defined with respect to the accepted observations $\mathbf{x}^k, k \in \mathcal{K}^+$, meaning that $\exists \mathcal{Q}_n \subseteq \mathbb{R}^{\phi_n}$, $\mathcal{Q}_n \neq \emptyset$ such that $\forall \hat{\mathbf{q}}_n \in \mathcal{Q}_n$, $g_n(\mathbf{x}; \hat{\mathbf{q}}_n)$ is concave and*

$$g_n(\mathbf{x}_k; \hat{\mathbf{q}}_n) \geq \mathbf{0} \quad \forall n \in \tilde{\mathcal{N}}, k \in \mathcal{K}^+.$$

Assumption 1 states that the structure of each nonlinear constraint permits parameter settings that make the FO problem convex and allows all accepted observations to be feasible for the constraint. This assumption ensures that the nonlinear constraints are well defined and that FO is convex. Similarly, the known constraints must also be well-defined with respect to the accepted observations, as stated in Assumption 2.

ASSUMPTION 2. *All accepted observations satisfy the known constraints, i.e.,*

$$\mathbf{x}^k \in \mathcal{X}, \quad \forall k \in \mathcal{K}^+.$$

Assumption 2 is not a limiting assumption in practice, because data can be pre-processed to ensure that there are no inconsistencies with respect to the known constraints. Through this pre-processing, we can also ensure that the labeling of accepted and rejected observations is free of contradictions. For instance, a solution cannot be accepted if an identical one is rejected in the dataset. Let \mathcal{H} be the convex hull of all accepted observations $\mathbf{x}^k, k \in \mathcal{K}^+$. The following assumption ensures the accepted and rejected data are not contradicting.

ASSUMPTION 3. *$\nexists k \in \mathcal{K}^-$ such that $\mathbf{x}^k \in \mathcal{H}, k \in \mathcal{K}^-$.*

Assumption 3 states that no rejected observation lies within the convex hull of all accepted observations. Together, Assumptions 1–3 ensure that the data and model are well defined and it is possible to construct a convex feasible region for FO. Because the objective function $f(\mathbf{x}; \mathbf{c})$ is known in FO, we can identify the points in the convex hull of all accepted observations that provide the best objective value in FO. Definition 1 characterizes such a point as the “preferred

solution”. An example of the preferred solution for a convex objective function is visualized in Figure 2, where the blue dashed lines indicate iso-cost lines of the objective function and \mathbf{x}^0 is the preferred solution. This concept is formally introduced in Definition 1.

DEFINITION 1. The *preferred* solution $\mathbf{x}^0 \in \mathbb{R}^m$ is defined as

$$\mathbf{x}^0 \in \arg \min_{\mathbf{x} \in \mathcal{H}} \{f(\mathbf{x}; \mathbf{c})\}.$$

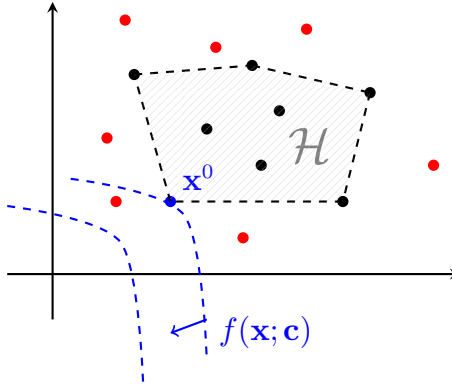


Figure 2 The preferred solution \mathbf{x}^0 has the best objective value among the convex hull of accepted observations.

Note that depending on the type of objective function and the shape of the convex hull \mathcal{H} , there may be multiple observations that satisfy the definition of a preferred solution, in which case, we arbitrarily label one of them as \mathbf{x}^0 . The preferred solution is not necessarily one of the observations, but it is always on the boundary of the convex hull of all observations.

The goal of this paper is to compute a set of linear and nonlinear constraints for the FO problem such that the accepted/rejected observations are inside/outside the inferred feasible region, respectively, and a preferred solution is an optimal solution for the FO model with the inferred feasible set. Hence, the intersection of the known constraints and the inferred constraints must include all the accepted observations and none of the rejected ones, providing a separation between the accepted and rejected points. In this paper, we will refer to such a set of inferred constraints as a “nominal set”, as formally defined in Definition 2. A simplified two-dimensional schematic of a nominal set is depicted in Figure 3.

DEFINITION 2. A convex set $\tilde{\mathcal{X}}$ is a *nominal* set if

$$\mathbf{x}^k \in \mathcal{X} \cap \tilde{\mathcal{X}} \quad \forall k \in \mathcal{K}^+,$$

$$\mathbf{x}^k \notin \mathcal{X} \cap \tilde{\mathcal{X}} \quad \forall k \in \mathcal{K}^-.$$

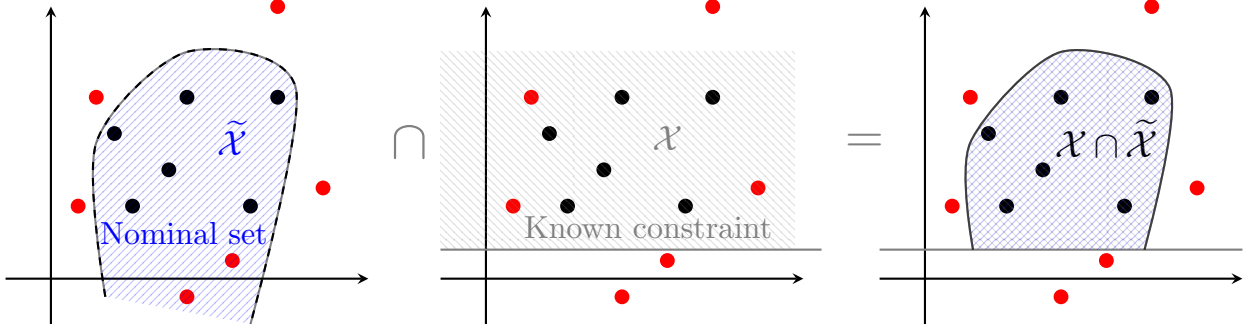


Figure 3 An illustration of the intersection of a nominal set and known constraints.

Hence, the goal of the inverse problem is to find constraint parameters $\mathbf{a}_\ell, b_\ell, \forall \ell \in \tilde{\mathcal{L}}$, and $\mathbf{q}_n, \forall n \in \tilde{\mathcal{N}}$ such that the resulting inferred feasible set $\tilde{\mathcal{X}}$ is a nominal set, and the preferred solution \mathbf{x}^0 is an optimal solution for

$$\begin{aligned} & \underset{\mathbf{x}}{\text{minimize}} \quad f(\mathbf{x}; \mathbf{c}) \\ & \text{subject to} \quad \mathbf{x} \in \mathcal{X} \cap \tilde{\mathcal{X}}. \end{aligned}$$

To impute such constraints, we propose a data-driven inverse optimization (DIO) formulation that imposes feasibility constraints on the accepted observations, ensures the infeasibility of the rejected points, and enforces optimality conditions on the preferred solution \mathbf{x}^0 . The DIO model can be written as follows.

$$\text{DIO :} \underset{\mathbf{a}, \mathbf{b}, \mathbf{q}, \lambda, \mu, y}{\text{Maximize}} \quad \mathcal{D} \left(\mathbf{q}_1, \dots, \mathbf{q}_{|\tilde{\mathcal{N}}|}, \mathbf{A}, \mathbf{b}; (\mathbf{x}^1, \dots, \mathbf{x}^{|\mathcal{K}|}) \right) \quad (2a)$$

$$\text{subject to} \quad g_n(\mathbf{x}^k; \mathbf{q}_n) \geq \mathbf{0}, \quad \forall k \in \mathcal{K}^+, n \in \tilde{\mathcal{N}}, \quad (2b)$$

$$\mathbf{a}'_\ell \mathbf{x}^k \geq b_\ell, \quad \forall k \in \mathcal{K}^+, \ell \in \tilde{\mathcal{L}} \quad (2c)$$

$$\nabla f(\mathbf{x}^0; \mathbf{c}) + \sum_{n \in \mathcal{N} \cup \tilde{\mathcal{N}}} \lambda_n \nabla g_n(\mathbf{x}^0, \mathbf{q}_n) + \sum_{\ell \in \mathcal{L} \cup \tilde{\mathcal{L}}} \mu_\ell \mathbf{a}_\ell = \mathbf{0}, \quad (2d)$$

$$\lambda_n g_n(\mathbf{x}^0, \mathbf{q}_n) = 0, \quad \forall n \in \mathcal{N} \cup \tilde{\mathcal{N}}, \quad (2e)$$

$$\mu_\ell (b_\ell - \mathbf{a}'_\ell x^0) = 0, \quad \forall \ell \in \mathcal{L} \cup \tilde{\mathcal{L}}, \quad (2f)$$

$$\mathbf{a}'_\ell \mathbf{x}^k \leq b_\ell - \epsilon + M y_{\ell k}, \quad \forall \ell \in \mathcal{L} \cup \tilde{\mathcal{L}}, k \in \mathcal{K}^-, \quad (2g)$$

$$g_n(\mathbf{x}^k; \mathbf{q}_n) \leq \mathbf{0} - \epsilon + M y_{nk}, \quad \forall n \in \mathcal{N} \cup \tilde{\mathcal{N}}, k \in \mathcal{K}^-, \quad (2h)$$

$$\sum_{i \in \mathcal{I}} y_{ik} \leq |\mathcal{I}| - 1, \quad \forall k \in \mathcal{K}^-, \quad (2i)$$

$$\mathbf{a}_\ell \in \mathcal{A}_\ell, b_\ell \in \mathcal{B}_\ell, \quad \forall \ell \in \tilde{\mathcal{L}}, \quad (2j)$$

$$\mathbf{q}_n \in \mathcal{Q}_n, \quad \forall n \in \tilde{\mathcal{N}}, \quad (2k)$$

$$\lambda_n, \mu_\ell \leq 0, \quad \forall n \in \mathcal{N} \cup \tilde{\mathcal{N}}, \ell \in \mathcal{L} \cup \tilde{\mathcal{L}}, \quad (2l)$$

$$y_{ik} \in \{0, 1\}, \quad \forall i \in \mathcal{I}, k \in \mathcal{K}^-. \quad (2m)$$

The objective function (2a) maximizes a measure of distance between the constraint parameters and the observations. An example of the objective function can be maximizing the total distance between the inferred constraints and all the infeasible observations using a desirable distance matrix \mathcal{D} . We provide more details on this objective function example in Section 3.3. Constraints (2b), (2c) enforce primal feasibility conditions. Constraints (2d) capture the stationarity conditions. Complementary slackness for the linear and nonlinear constraints of FO are captured in (2e) and (2f), respectively. Constraints (2g)–(2i) ensure that at least one constraint is violated by each of the rejected observations. Constraints (2j)–(2k) provide a set of desirable conditions on the coefficients of the imputed constraints such as normalization or convexity conditions. As an optional step, any other desirable condition on the parameters can also be included in \mathcal{Q} , and similar conditions on the linear constraint parameters can also be considered as $\mathbf{a}_\ell \in \mathcal{A}, b_\ell \in \mathcal{B}$. Lastly, constraints (2l)–(2m) indicate sign and binary declarations.

We next show that any optimal solution produced by the DIO model exhibits the desired properties of an inferred feasible region for FO.

PROPOSITION 1. *Any feasible solution of DIO corresponds to a nominal set $\tilde{\mathcal{X}}$ such that $\mathbf{x}^0 \in \arg \min_{\mathbf{x} \in \mathcal{X} \cap \tilde{\mathcal{X}}} \{f(\mathbf{x}; \mathbf{c})\}$.*

As Proposition 1 states, any solution of DIO has the properties of a nominal feasible set for FO and makes \mathbf{x}^0 optimal for the forward problem. To fulfill this requirement, DIO inserts at least one conflicting constraint per rejected observation such that the rejected observation becomes infeasible for FO while ensuring none of the accepted observations are cut off. Assuming that the forward model allows us to infer as many constraints needed to do so, then it is always possible to find a solution for DIO.

PROPOSITION 2. *For sufficiently large $|\tilde{\mathcal{L}}| + |\tilde{\mathcal{N}}|$, DIO is guaranteed to be feasible.*

Given that Proposition 2 states that DIO is feasible when the number of inferred constraints is sufficiently large, we next construct an upper bound on the minimum number of constraints needed to make DIO feasible. Depending on the number of rejected observations and their spatial distribution, a small number of constraints may be sufficient to cut off a large number of rejected observations. However, in the worst case, we would need one constraint per rejected observation to guarantee that each rejected point is infeasible for FO while ensuring the feasibility of all accepted points. We also need at least one inferred constraint ensuring that the preferred solution \mathbf{x}^0 is optimal for FO. Remark 1 provides a bound for the number of inferred constraints required for DIO.

REMARK 1. An upper bound to the minimum number of required constraints in DIO is $|\mathcal{K}^-| + 1$.

We note again that one constraint may serve multiple purposes, which would result in a lower number of constraints needed in practical settings. For instance, a single constraint may cut a large number of rejected points out of the inferred feasible region.

The FO problem considered in this paper is a general convex nonlinear problem that may be relatively hard to solve, but global optimality is guaranteed due to its convexity and specific classes of convex problems can be solved efficiently (Boyd and Vandenberghe 2004). The proposed DIO model for constraint inference adds extra levels of complexity to the FO model, mainly due to the addition of KKT conditions of complementary slackness and stationarity, which are nonlinear

and not necessarily convex. It also adds binary variables and additional constraints to account for the infeasibility of rejected points. Therefore, the proposed DIO model of formulation (2) can be a very complex mixed-integer nonlinear nonconvex problem for which there is no optimality guarantee and we found that commercial solvers often fail to find any good-quality solutions even for small problem instances. In Section 3, we propose a method for mitigating the complexity of the proposed inverse problem.

3. Mitigating Inverse Problem Complexity

For inferring linear FO constraints, Ghobadi and Mahmoudzadeh (2021) proposed a tractable reformulation of the inverse model that leverages the structure of a class of solutions to provide an equivalent tractable reformulation that can be reduced to a linear program. Using the concept of optimality in linear programming, they add a linear half-space as a known constraint that would eliminate the need for writing strong duality and dual feasibility conditions in the inverse model. Hence, at the expense of adding one constraint to the set of known constraints, the complexity of their inverse model can potentially be reduced to an LP.

In this section, we generalize the methodology of Ghobadi and Mahmoudzadeh (2021) to convex FO models and demonstrate that a data-driven constraint can be derived and added to the FO formulation to replace optimality conditions. We show that the inclusion of this additional constraint can simplify the resulting inverse formulation. In what follows, we first introduce a few definitions and discuss preliminaries for constructing the reformulation. We then discuss the properties of an optimal inverse solution and provide problem-specific sufficient optimality conditions that are simpler than the KKT criteria. Lastly, we present a reduced reformulation of the inverse problem, which is easier to solve than the original DIO model.

3.1. Preliminaries and Definitions

One of the key complexities of the DIO formulation is the inclusion of nonlinear KKT conditions for stationarity and complementary slackness, which ensure the optimality of the preferred solution.

Recall that the preferred solution \mathbf{x}^0 is optimal for FO, meaning that it has a better objective value for $f(\mathbf{x}; \mathbf{c})$ than any other accepted observation. This means that $f(\mathbf{x}^0; \mathbf{c}) \leq f(\mathbf{x}^k; \mathbf{c})$, $\forall k \in \mathcal{K}^+$. In a simplified two-dimensional setting, if we draw the iso-cost objective function curve at $f(\mathbf{x}; \mathbf{c}) = f(\mathbf{x}^0; \mathbf{c})$, all accepted observations fall on one side of this curve. Definition 3 formally defines this space on one side of the curve as the sublevel set of the objective function at the preferred solution.

DEFINITION 3. The subspace \mathcal{V} is a \mathbf{x}^0 -sublevel set of $f(\mathbf{x}; \mathbf{c})$ at \mathbf{x}^0 defined as

$$\mathcal{V} = \{\mathbf{x} \mid f(\mathbf{x}; \mathbf{c}) \geq f(\mathbf{x}^0; \mathbf{c})\}.$$

Note that the sublevel space \mathcal{V} always contains all accepted observations, because any point $\hat{\mathbf{x}} \notin \mathcal{V}$ would have a better objective value than \mathbf{x}^0 , i.e., $(\hat{\mathbf{x}}; \mathbf{c}) < (\mathbf{x}; \mathbf{c})$, which contradicts with \mathbf{x}^0 being the preferred solution. When $(\mathbf{x}; \mathbf{c})$ is convex, the sublevel set \mathcal{V} is either non-convex or a half-space, when $f(\mathbf{x}; \mathbf{c})$ is nonlinear or linear in \mathbf{x} , respectively. When $f(\mathbf{x}; \mathbf{c})$ is not linear, the sublevel set is a nonconvex set that contains all feasible observations and has \mathbf{x}^0 on its boundary. The preferred solution is also on the boundary of the tangent half-space to the sublevel set, which is one side of a hyperplane that is tangent to $f(\mathbf{x}; \mathbf{c})$ at \mathbf{x}^0 . Simplified schematics of a sublevel set and its tangent half-space are shown in Figure 4. The tangent half-space is formally introduced in Definition 4.

DEFINITION 4. The tangent half-space \mathcal{C} to the sublevel set of $f(\mathbf{x}; \mathbf{c})$ at \mathbf{x}^0 is defined as

$$\mathcal{C} = \{\mathbf{x} \in \mathbb{R}^n \mid (\nabla f(\mathbf{x}^0; \mathbf{c}))' \mathbf{x} \geq f(\mathbf{x}^0; \mathbf{c})\}.$$

It can be seen that if $f(\mathbf{x}; \mathbf{c})$ is linear, the tangent half-space is equivalent to the sublevel set of $f(\mathbf{x}; \mathbf{c})$ at \mathbf{x}^0 , i.e., $\mathcal{C} = \mathcal{V}$. In the rest of this paper, we use \mathcal{C} to denote the tangent half-space of the sublevel set of $f(\mathbf{x}; \mathbf{c})$ at \mathbf{x}^0 , for brevity. With these definitions in place, we next discuss the properties of DIO solutions, which will allow us to derive a reduced reformulation that enforces optimality conditions on \mathbf{x}^0 without explicitly incorporating KKT conditions.

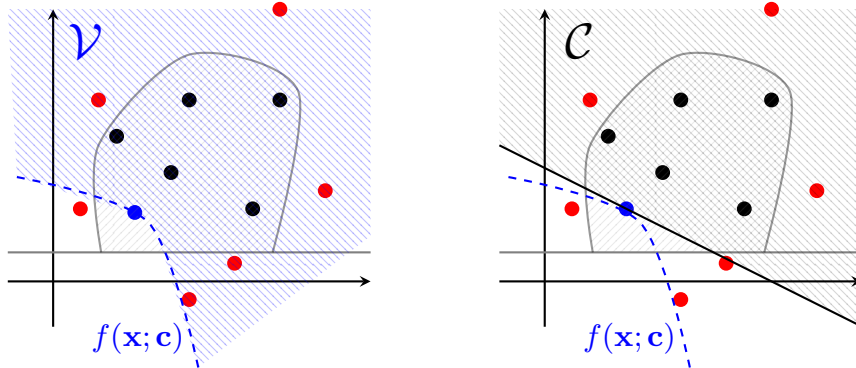


Figure 4 The sublevel set of $f(\mathbf{x}; \mathbf{c})$ (left) and its tangent half-space (right) at \mathbf{x}^0 .

3.2. Reduced Formulation

In this section, we use the theoretical properties of a DIO solution to enforce optimality conditions through a reduced reformulation that is less complex than the original DIO model. For brevity of notations, we refer to any feasible region that is inferred using the DIO model as an *imputed feasible set* for the forward problem. Given the properties of DIO solution outlined in Proposition 1, Definition 5 characterizes an imputed feasible set for FO.

DEFINITION 5. Any convex nominal set $\mathcal{S} = \mathcal{X} \cap \tilde{\mathcal{X}}$ such that $\mathbf{x}^0 \in \arg \min_{\mathbf{x} \in \mathcal{X} \cap \tilde{\mathcal{X}}} \{f(\mathbf{x}; \mathbf{c})\}$ is an *imputed set* for FO.

We note that different DIO solutions may result in the same imputed feasible set since the imputed set is a geometric representation of the feasible region, as opposed to an algebraic one. For instance, in a DIO solution, multiplying the coefficients of a linear constraint by a constant would result in a different solution, which may even be infeasible for DIO, but it would represent the same imputed feasible set for FO.

Recall the definition of tangent half-space \mathcal{C} of the sublevel set of $f(\mathbf{x}; \mathbf{c})$ at \mathbf{x}^0 in Definition 3. It can be shown that any imputed feasible set as defined in Definition 5 is always contained within the tangent half-space \mathcal{C} . This property is detailed in Proposition 3.

PROPOSITION 3. *If a $\mathcal{S} = \mathcal{X} \cap \tilde{\mathcal{X}}$ is an imputed set for FO then $\mathcal{S} \subseteq \mathcal{C}$.*

Figure 5 shows the intuition behind Proposition 3 which states any imputed set for FO must be contained within the tangent half-space \mathcal{C} . Consider the convex nominal set \mathcal{S} denoted by the

dashed green area, which is not contained within \mathcal{C} . Then \mathcal{S} must contain points outside of \mathcal{C} that are either in $\mathcal{V} \setminus \mathcal{C}$ or in the complement of \mathcal{V} . If \mathcal{S} contains $\hat{\mathbf{x}}' \notin \mathcal{V}$, then it cannot be an imputed set, by definition, since $\hat{\mathbf{x}}'$ dominates \mathbf{x}^0 and hence $\mathbf{x}^0 \notin \arg \min_{\mathbf{x} \in \mathcal{S}} \{f(\mathbf{x}; \mathbf{c})\}$. If, \mathcal{S} contains a point $\hat{\mathbf{x}} \in \mathcal{V} \setminus \mathcal{C}$, then because $f(\mathbf{x}; \mathbf{c})$ is convex, there exists a convex combination of \mathbf{x}^0 and $\hat{\mathbf{x}}$ that dominates \mathbf{x}^0 and hence, again, $\mathbf{x}^0 \notin \arg \min_{\mathbf{x} \in \mathcal{S}} \{f(\mathbf{x}; \mathbf{c})\}$, which contradicts the definition of an imputed set. Proposition 3 provides a guideline for constructing an imputed feasible set by intersecting any convex nominal set with the tangent half-space \mathcal{C} , as outlined in Proposition 4.

PROPOSITION 4. *For any convex nominal set \mathcal{S} , the set $\mathcal{S} \cap \mathcal{C}$ is an imputed feasible set.*

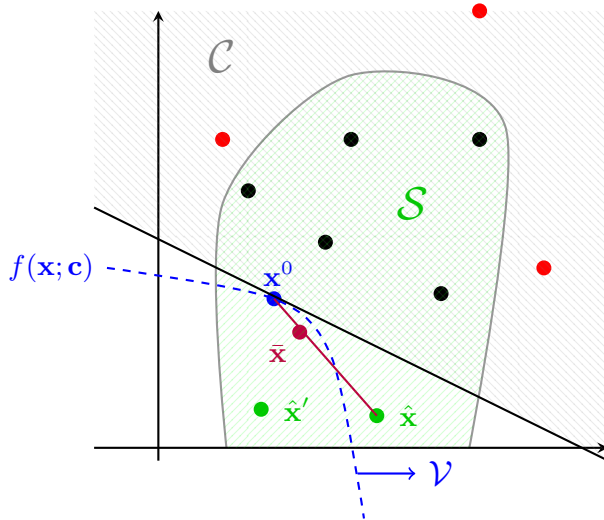


Figure 5 A convex nominal set $\mathcal{S} \not\subseteq \mathcal{C}$, to show the intuition behind Proposition 3

Proposition 4 illustrates that the optimality condition on \mathbf{x}^0 can always be guaranteed if \mathcal{C} is used as one of the constraints in shaping the imputed feasible set. Because any imputed feasible set must be a subset of the tangent half-space \mathcal{C} , as shown in Proposition 3, the addition of \mathcal{C} does not exclude or cut any possible imputed sets for FO. Hence, instead of searching for a nominal set that satisfies the optimality on \mathbf{x}^0 , we can add the tangent half-space \mathcal{C} as one of the known constraints for FO, thereby, always guaranteeing that \mathbf{x}^0 will be the optimal solution of FO for any inferred feasible set. This additional constraint allows us to relax the KKT conditions on the optimality of \mathbf{x}^0 in the DIO formulation and derive a reduced formulation, presented in Theorem 1.

THEOREM 1. *When \mathcal{C} is appended to the known constraints of FO, then solving DIO is equivalent to solving the following reduced model:*

$$\mathbf{RDIO:} \quad \underset{\mathbf{a}, \mathbf{b}, \mathbf{q}, \mathbf{y}}{\text{Maximize}} \quad \mathcal{D} \left(\mathbf{q}_1, \dots, \mathbf{q}_{|\tilde{\mathcal{N}}|}, \mathbf{A}, \mathbf{b}; (\mathbf{x}^1, \dots, \mathbf{x}^{|\mathcal{K}|}) \right) \quad (3a)$$

$$\text{subject to} \quad g_n(\mathbf{x}^k; \mathbf{q}_n) \geq \mathbf{0}, \quad \forall k \in \mathcal{K}^+, n \in \tilde{\mathcal{N}} \quad (3b)$$

$$\mathbf{a}'_\ell \mathbf{x}^k \geq b_\ell, \quad \forall k \in \mathcal{K}^+, \ell \in \tilde{\mathcal{L}} \quad (3c)$$

$$\mathbf{a}_\ell \mathbf{x}^k \leq b_\ell - \epsilon + M y_{\ell k}, \quad \forall \ell \in \mathcal{L} \cup \tilde{\mathcal{L}}, k \in \mathcal{K}^- \quad (3d)$$

$$g_n(\mathbf{x}^k; \mathbf{q}_n) \leq \mathbf{0} - \epsilon + M y_{nk}, \quad \forall n \in \mathcal{N} \cup \tilde{\mathcal{N}}, k \in \mathcal{K}^- \quad (3e)$$

$$\sum_{i \in \mathcal{I}} y_{ik} \leq |\mathcal{I}| - 1, \quad \forall k \in \mathcal{K}^- \quad (3f)$$

$$\mathbf{a}_\ell \in \mathcal{A}_\ell, b_\ell \in \mathcal{B}_\ell \quad \forall \ell \in \tilde{\mathcal{L}} \quad (3g)$$

$$\mathbf{q}_n \in \mathcal{Q}_n, \quad \forall n \in \tilde{\mathcal{N}} \quad (3h)$$

$$y_{ik} \in \{0, 1\}, \quad \forall i \in \mathcal{I}, k \in \mathcal{K}^- \quad (3i)$$

We note that RDIO is always feasible because it is a relaxed version of DIO with fewer constraints, and we know from Proposition 2 that DIO is always feasible. Based on Theorem 1, to find an imputed feasible set, we can simply find a nominal feasible set and super-impose the known constraints including the tangent halfspace of the sublevel set of $f(\mathbf{x}; \mathbf{c})$ at the preferred solution \mathbf{x}^0 .

COROLLARY 1. *RDIO infers unknown constraints $\tilde{\mathcal{X}}$ that shape a nominal feasible set for FO such that \mathbf{x}^0 is an optimal solution of*

$$\underset{\mathbf{x}}{\text{minimize}} \quad f(\mathbf{x}; \mathbf{c}), \quad (4a)$$

$$\text{subject to} \quad \mathbf{x} \in \mathcal{C} \cap \mathcal{X} \cap \tilde{\mathcal{X}}. \quad (4b)$$

Corollary 1 provides a method for reducing the complexity of the DIO model. In what follows, we provide a numerical example that illustrates how an imputed feasible set can be constructed using Corollary 1. In this small numerical example, the solution is constructed by manual inspection.

EXAMPLE 1. Let $f(\mathbf{x}; \mathbf{c}) = x_1^2 + x_2^2$ be the convex objective function of FO, and let the feasible and infeasible observations be the black and red points shown in Figure 6, respectively. The preferred solution can be identified based on Definition 1 and is shown on the figure as \mathbf{x}^0 . The sublevel set of $f(\mathbf{x}; \mathbf{c})$ at \mathbf{x}^0 is denoted as \mathcal{V} and can be written as $\mathcal{V} = \{\mathbf{x} \in \mathbb{R}^2 \mid x_1^2 + x_2^2 \geq 2\}$, which is the outside of the dashed circle passing through \mathbf{x}^0 . Assume that a known constraint is $2x_1 - 3x_2 \leq 4$ for which the corresponding side of the inequality is shown by \mathcal{X} in Figure 6.

A possible nominal feasible set for FO is $\tilde{\mathcal{X}} = \{(x_1, x_2) \in \mathbb{R}^2 \mid (x_1 - 2)^2 + 2(x_2 - 2)^2 \leq 6\}$ and depicted in Figure 6 in the green dashed area. Note that the intersection of this nominal set and the known constraint, i.e., $\mathcal{X} \cap \tilde{\mathcal{X}}$, only includes all accepted observations and exclude all the rejected observations. However, it does not have the preferred solution \mathbf{x}^0 and hence, would not make \mathbf{x}^0 to be optimal for FO. On the contrary, the tangent half-space \mathcal{C} allows for \mathbf{x}^0 to be a candidate optimal solution for FO when added as a known constraint for FO. Hence, $\tilde{\mathcal{X}} \cap \mathcal{X} \cap \mathcal{C}$ is an imputed feasible set for FO as it satisfies the properties outlined in Definition 5. \triangle

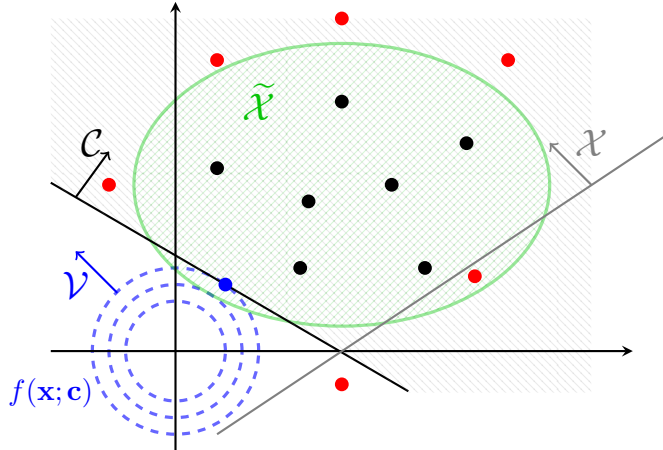


Figure 6 Illustration of the nominal and imputed sets, the sublevel set of the objective function, and the tangent hyperplane in Example 1.

The RDIO model eliminates the need for explicitly writing the stationarity and complementary slackness constraints because the inclusion of the tangent half-space \mathcal{C} makes them redundant for the DIO model. Because \mathcal{C} is a tangent half-space of the sublevel set of $f(\mathbf{x}; \mathbf{c})$ at the preferred

solution \mathbf{x}^0 , its inclusion ensures that the resulting inferred feasible region is an imputed feasible set. The only constraints that are required to remain in the RDIO model are those that ensure the imputed constraints form a nominal solution that includes all accepted observations and none of the rejected ones. Therefore, the size of the RDIO problem is considerably lower than that of the DIO problem, and it relaxes a large number of nonconvex nonlinear constraints. A comparison of the number of variables and constraints in the DIO and RDIO models is provided in Table 1.

	Type	Model	Number
Variables	Continuous	DIO	$(m+2) \tilde{\mathcal{L}} + (\phi+1) \tilde{\mathcal{N}} + \mathcal{N} + \mathcal{L} $
		RDIO	$(m+1) \tilde{\mathcal{L}} + \phi \tilde{\mathcal{N}} $
	Binary	DIO	$(\mathcal{N} + \mathcal{L} + \tilde{\mathcal{N}} + \tilde{\mathcal{L}}) \mathcal{K}^- $
		RDIO	$(\mathcal{N} + \mathcal{L} + \tilde{\mathcal{N}} + \tilde{\mathcal{L}}) \mathcal{K}^- $
Constraints	Linear	DIO	$ \tilde{\mathcal{L}} (\mathcal{K}^+ + 1) + (\mathcal{L} + 1) \mathcal{K}^- $
		RDIO	$ \tilde{\mathcal{L}} (\mathcal{K}^+ + 1) + (\mathcal{L} + 1) \mathcal{K}^- $
	Nonlinear	DIO	$ \tilde{\mathcal{N}} (\mathcal{K}^+ + \mathcal{K}^- + 1) + \mathcal{N} (\mathcal{K}^- + 1) + m$
		RDIO	$ \tilde{\mathcal{N}} (\mathcal{K}^+ + \mathcal{K}^-) + \mathcal{N} \mathcal{K}^- $

Table 1 Comparison of the number of variables and constraints in the DIO and RDIO models.

Table 1 shows that the RDIO model has fewer continuous variables and nonlinear constraints compared to the DIO model. The nonlinear constraints that remain in RDIO primal feasibility constraints ($g_n(\mathbf{x}; \mathbf{q}) \geq$) which are nonlinear in \mathbf{x} , but may be linear (or be linearized) in \mathbf{q}_n , which is the decision variable in RDIO. Particularly, if the FO is linear, then the corresponding RDIO model can also be linear if a linear distance metric is used in the objective function. In what follows, we discuss one example of a distance metric that can be used in the RDIO model.

3.3. Example of Distance Metric

The objective function in DIO and RDIO maximizes a non-negative distance metric between the inferred constraints and the observations. In this section, we provide an example of such a distance metric and write the complete DIO formulation based on it, which will be used in the case study presented in Section 4.

We consider an objective that aims to find constraints that are as far as possible from the rejected observations and as close as possible to the accepted ones. To formulate this objective, we maximize the maximum distance between the inferred constraints that exclude each of the rejected observation, $\mathbf{x}^k, k \in \mathcal{K}^-$, from the inferred feasible set. That is, among the constraints that make each rejected observation infeasible, we select the constraint furthest away from the rejected observation and push it as close to the accepted observations as possible. Hence, we define \mathcal{D} as

$$\mathcal{D}(\mathbf{q}_1, \dots, \mathbf{q}_{|\tilde{\mathcal{N}}|}, \mathbf{A}, \mathbf{b}; (\mathbf{x}^1, \dots, \mathbf{x}^{|\mathcal{K}|})) = \sum_{k \in \mathcal{K}^-} \max \left\{ \max_{\ell \in \mathcal{L}} \{d_{\ell k}([\mathbf{a}_\ell, b_\ell], \mathbf{x}^k)\}, \max \{d_{nk}(\mathbf{q}_n, \mathbf{x}^k)\} \right\},$$

where d_{ik} is the distance between the imputed constraint i and the rejected observation $k \in \mathcal{K}^-$ defined as the slack of the corresponding constraint. This objective can be linearized using a set of additional constraints as shown in **RDIO₁**.

$$\mathbf{RDIO}_1 : \underset{\mathbf{a}, \mathbf{b}, \mathbf{q}, y}{\text{Maximize}} \quad \sum_{k \in \mathcal{K}^-} z_k \quad (5a)$$

$$\text{subject to} \quad d_{nk} \geq -g_n(\mathbf{x}^k; \mathbf{q}_n) \quad \forall \in \tilde{\mathcal{N}}, k \in \mathcal{K}^- \quad (5b)$$

$$d_{nk} \leq -g_n(\mathbf{x}^k; \mathbf{q}_n) + M y_{nk} \quad \forall \in \tilde{\mathcal{N}}, k \in \mathcal{K}^- \quad (5c)$$

$$d_{\ell k} \geq b_\ell - \mathbf{a}'_\ell \mathbf{x}_k \quad \forall \ell \in \tilde{\mathcal{L}}, k \in \mathcal{K}^- \quad (5d)$$

$$d_{\ell k} \leq b_\ell - \sum_{m \in M} \mathbf{a}'_\ell \mathbf{x}_k + M y_{\ell k} \quad \forall \ell \in \tilde{\mathcal{L}}, k \in \mathcal{K}^- \quad (5e)$$

$$d_{ik} \leq M(1 - y_{ik}) \quad \forall i \in \tilde{\mathcal{N}} \cup \tilde{\mathcal{L}}, k \in \mathcal{K}^- \quad (5f)$$

$$d_{ik} \geq \epsilon(1 - y_{ik}) \quad \forall i \in \tilde{\mathcal{N}} \cup \tilde{\mathcal{L}}, k \in \mathcal{K}^- \quad (5g)$$

$$z_k \leq d_{ik} + M p_{ik} \quad \forall i \in \tilde{\mathcal{N}} \cup \tilde{\mathcal{L}}, k \in \mathcal{K}^- \quad (5h)$$

$$p_{ik} \leq |\mathcal{I}| - 1 \quad \forall i \in \tilde{\mathcal{N}} \cup \tilde{\mathcal{L}}, k \in \mathcal{K}^- \quad (5i)$$

$$p_{ik} \geq y_{ik} \quad \forall i \in \tilde{\mathcal{N}} \cup \tilde{\mathcal{L}}, k \in \mathcal{K}^- \quad (5j)$$

$$(3c) - (3i) \quad (5k)$$

$$d_{\ell k} \geq 0 \quad (5l)$$

Constraints (5b)–(5g) find the slack distance between each rejected point and each constraint. Constraints (5h)–(5j) find the maximum distance of each constraint that make each point infeasible, and the objective (5a) maximizes this maximum distance. The original primal feasibility constraints of the RDIO model are also enforced. Note that this specific distance model only requires the addition of linear constraints and binary variables, so if the FO is a linear problem, the corresponding RDIO problem will be a linear integer problem. Any other metric of interest can also be used in the objective, but for simplicity, we will use this linear metric in the case study in Section 4.

4. Case Study: Standardizing Clinical Radiation Therapy Guidelines

In this section, we test the proposed methodology using a case study on standardizing radiation therapy treatment planning guidelines for breast cancer patients. We first introduce the case and the problem in the context of radiation therapy. Next, we describe the data and experimental setup. Lastly, we present and discuss the results and provide practical insights.

4.1. Case description

Breast cancer is the most widely diagnosed type of cancer in women worldwide. The cancerous tumor is often removed, leaving behind a cavity, and radiation treatment is subsequently prescribed to eliminate any remaining cancer cells. Tangential Intensity-modulated radiation therapy (IMRT) is a treatment modality often used as part of the treatment for most breast cancer patients. In tangential IMRT, two opposing beams that are tangent to the external body of the patient are used to deliver radiation to the breast tissue. The main organ at risk in breast cancer IMRT is the heart, particularly when the left breast is being irradiated (Mahmoudzadeh et al. 2015). The goal is to

find the radiation beam configurations from each angle such that the clinical target volume (CTV) inside the breast is fully irradiated and the heart is spared from radiation as much as possible. Figure 7 shows a computed tomography (CT) scan of a breast cancer patient along with the two tangential beams and the contours showing the organs at risk.

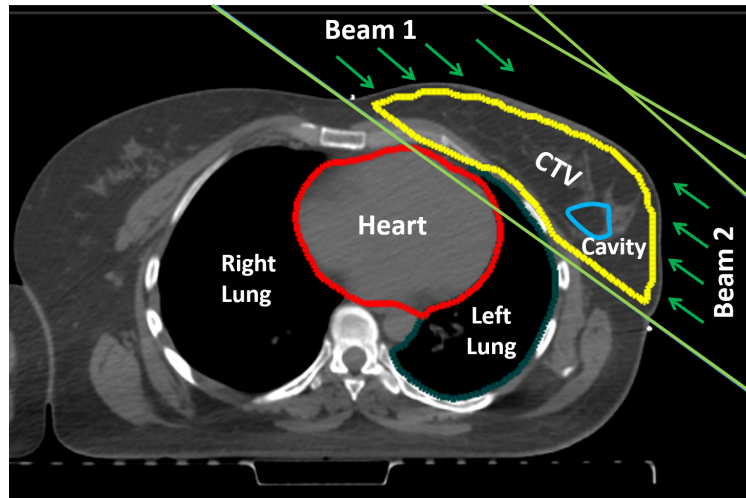


Figure 7 Computed Tomography (CT) scan of a breast cancer patient with important organs delineated. Image adapted from [Mahmoudzadeh et al. \(2015\)](#).

There are a set of acceptability guidelines in breast cancer treatment planning, which involve clinical dose-volume criteria on the CTV and the heart. A dose-volume criterion is a clinical metric that calculates the dose threshold to a certain fraction of an organ measured in units of radiation dose, Gray (Gy). For instance, the prescribed dose for the CTV is 42.4 Gy and at least 99% of the CTV must receive lower than 95% of the prescribed dose for a plan to be accepted. That is, if the body is discretized into three-dimensional cubes called voxels, then the 95% quantile of the voxels must receive a dose of $42.4 \times 0.95 = 40.28$ Gy or higher. Similarly, at most 0.5% of the CTV can receive a dose higher than 108% of the prescribed dose, which means the dose to upper 0.5% quantile of the CTV must be lower than $1.08 \times 42.4 = 45.792$. There are also upper bounds on the dose delivered to the heart, where the highest-dosed 10 cc and 25 cc volume of the heart must receive a dose lower than 90% and 50% of the prescribed dose, respectively.

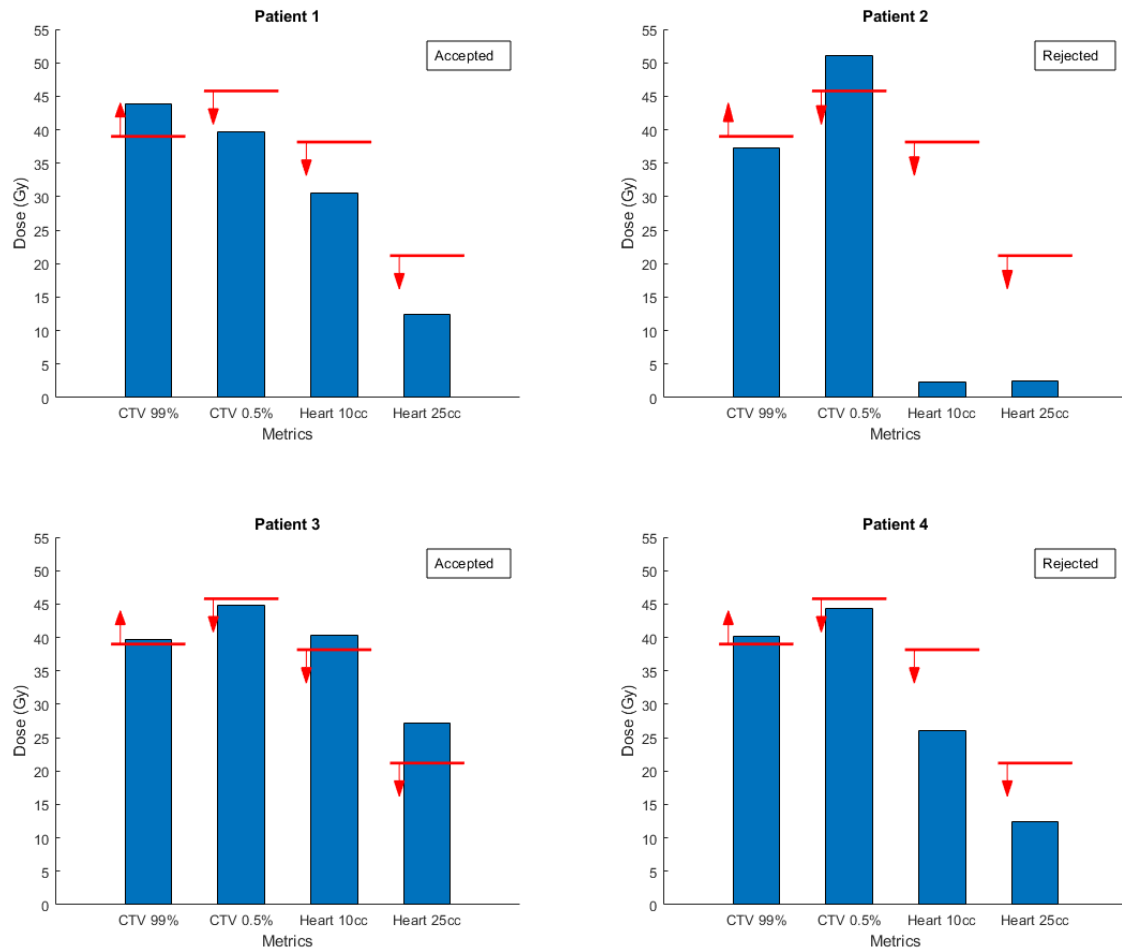


Figure 8 Examples of accepted/rejected treatment plans. The guidelines are indicated with (red) lines on the bars and arrows indicate the direction of bounds.

These clinical dose-volume guidelines are used as a base reference for planning, but acceptance or rejection of the plan is at the discretion of oncologists, based on each patient's specific case. Figure 8 shows the clinical guidelines and the metric values for four different patients that are labeled as accepted or rejected. It can be seen that the plan for Patient 1 and Patient 3 are accepted, while the plan for Patient 1 meets the guidelines but the plan for Patient 3 is violating two of the dose-volume metrics on the heart. On the contrary, the plan for Patients 2 is rejected because it does not meet the guidelines, but the plan Patient 4 is also rejected even though it meets all the guidelines.

In this section, we consider a forward optimization problem that inputs a set of treatment plans and determines which ones are feasible or infeasible based on a set of constraints that impose limitations on a given clinical metrics. The FO finds the optimal plan among the feasible set, according to a known objective function. In this case study, we consider the objective of minimizing the overall dose to the entire body to reduce any unnecessary radiation exposure. The inverse model then inputs a set of past patient treatments that are labeled as accepted or rejected and infers a set of constraints that correctly classify the accepted and rejected plans as feasible and infeasible, respectively, and makes a preferred treatment plan optimal for the corresponding FO problem. We assume that there are no known constraints in FO, and for simplicity of computations, consider that all constraints are linear, which is relevant in practical settings for radiation therapy, since dose-volume criteria for breast cancer can be re-written as linear constraints (Chan et al. 2014a).

4.2. Data and Experimental setup

To set up the experiment, we used historical plans for 5 breast cancer datasets and perturbed the radiation dose of each of these 5 plans to generate 20 simulated plans based on each of these datasets. Then, we calculated 16 clinical dose metrics for each of these 105 patient datasets including maximum and minimum dose to different regions as well as dose-volume values for the CTV, the cavity, the heart, and the lung. Each of these plans was then labeled as accepted or rejected based on a set of expert-knowledge criteria that did not match the guidelines. A summary of the data is provided in Figure 9 where the error bars show the range of each metric for all patients in that category. Note that four of the calculated metrics match the guidelines (CTV 99%, CTV 0.5%, Heart 10cc, and Heart 25cc). The data visualization shows that there is no clear separation between accepted and rejected plans and the underlying logic behind the acceptance/rejection decision cannot be inferred by looking at these metrics. Specific patient examples from this dataset were also previously shown in Figure 8.

To test the prediction accuracy of the proposed inverse methodology, we randomly divided the data into training and testing sets. We used the training set, including both accepted and rejected

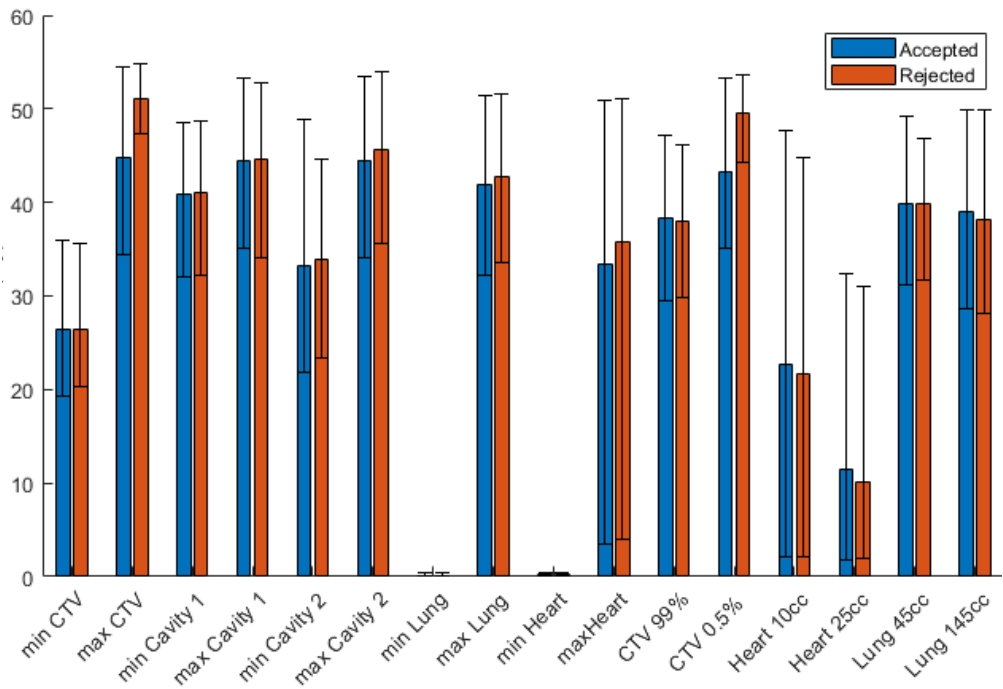


Figure 9 Visualization of a set of metrics calculated for all accepted and rejected plans. The errorbars show the range of each calculated metric across all plans in each category.

plans, as input to the inverse model and inferred 10 constraints for the forward problem. We then used the testing set to validate the results and to check whether the inferred constraints can accurately predict which plans in the testing set are accepted or rejected. We validated the out-of-sample prediction by calculating the accuracy (% correct prediction), precision: (% correct acceptance prediction), specificity (% correct rejection identified), recall (% correct acceptance identified), F1 Score (harmonic average of recall and precision). The results are provided in Section 4.3

4.3. Results

We first tested the model using a 60/40 random split for training/testing, ran the result 50 times, and computed the average and the range for each of the metrics. Figure 10 shows that the inverse model performs well with an average of above 95% and up to 100% across all metrics. The lowest metric was specificity at 95% which we believe was due to the low number of rejected observations in our datasets.

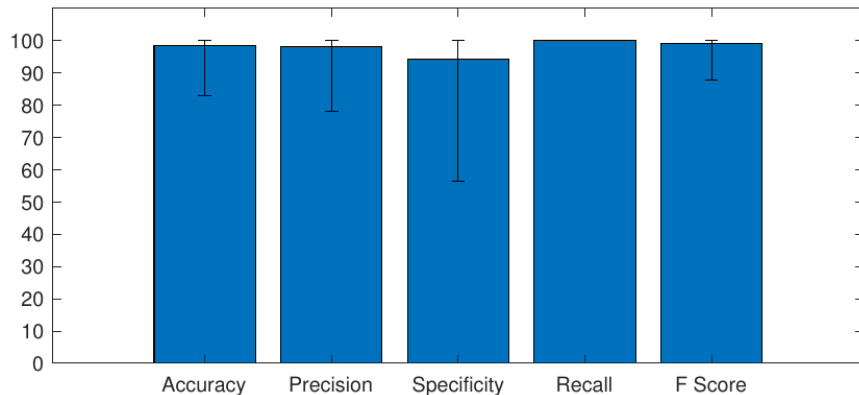


Figure 10 Out-of-sample performance of the inverse model using a 60/40 split for training/testing.

We next tested the sensitivity of the method to training size. Figure 11 illustrates the trends of each metric when the training size is varied between 20% to 80% in increments of 10%, with 250 random splits in each size. The x-axis shows the % of the data that was used for training (the rest used for testing), and the y-axis shows how each metric performed (on average). The results show that the method works well across the board, even when training on only 20% of the available data. We see a slight dip right before the 50-50 split but it picks up again when we pass the ratio. While there is always randomness, the methods seem to consistently obtain good results on average (with all metrics above 95%) at a 60-40 split. Note that if we train too much, the risk of overfitting increases and the out-of-sample result may suffer, which for this case study seems to happen at around 70-80% and upward. Even in the worst case, our recall and F1 scores are above 90%.

5. Discussions and Conclusions

In summary, this paper provides an inverse optimization framework that inputs both accepted and rejected observations and imputes a feasible region for a convex forward problem. The proposed inverse model is a complex nonlinear formulation; therefore, using the properties of the constructed solutions, we propose a reduced reformulation that mitigates some of the problem complexity by rendering a set of optimality conditions redundant.

We consider the problem of radiation therapy treatment planning to infer the implicit clinical guidelines that are utilized in practice based on historically-approved plans. Using realistic patient

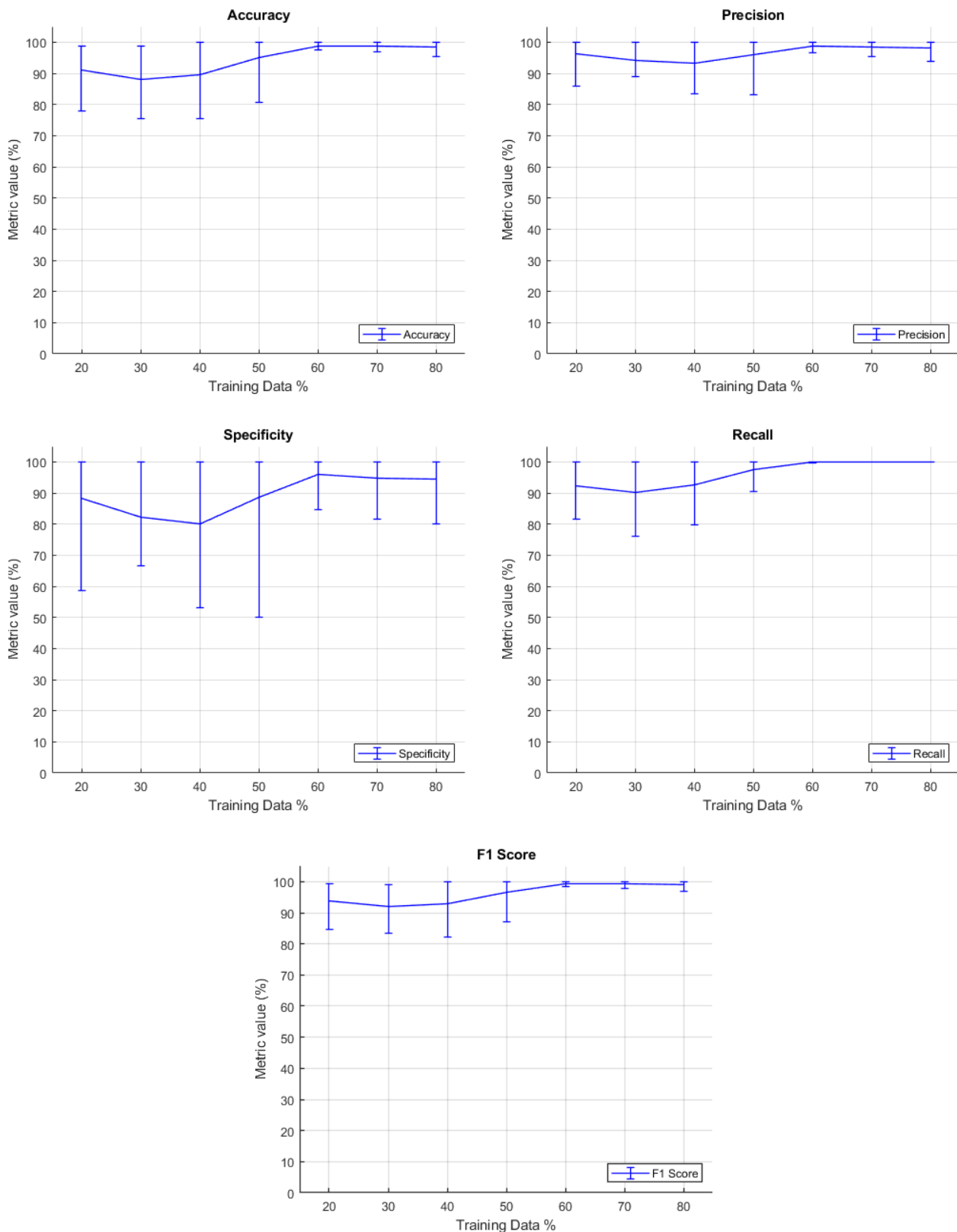


Figure 11 Sensitivity of different metrics with respect to the proportion of training data

datasets, we divide the data into training and testing sets and use our inverse models to derive a feasible region for accepted plans such that rejected plans are infeasible. Our results show that our obtained feasible region (i.e., the underlying clinical guidelines) performs with 95% accuracy in predicting the accepted and rejected treatment plans in out-of-sample data, on average. The results also highlight an interesting property of IO models that even with a small size of training data, high accuracy can be obtained. This characteristic, perhaps one of the advantages of IO compared to conventional machine learning methods, is due to the fact that IO models have a predetermined optimization structure.

In radiation therapy, implementing our methodology results in standardized clinical guidelines and infers the true underlying criteria based on which the accept/reject decisions are made. This information allows planners to generate higher-quality initial plans that, in turn, result in better patient care through personalized treatment plans. It also streamlines the planning process by reducing the number of times a plan is rejected and sent back for corrections. The standardization of the guidelines reduces variability, and potentially human errors, among clinicians and institutes, and enables personalized guidelines for patient subpopulations.

Given the data-driven nature of our framework, data quality and pre-processing can impact the size of our models and the quality of the obtained solutions. A simple pre-processing method can potentially reduce the size of the observations by identifying and removing those observations that are rendered infeasible by the known constraints. A reduction in the number of these infeasible observations can largely improve the complexity and size of the inverse problem by reducing the required number of inferred constraints required. Any redundant accepted or rejected observations (e.g., observation points with a distance less than a given threshold from each other) or outliers can be removed from the set of observations using the data cleaning method of choice. We assume that the data is well-defined for the FO problem, and those data points that contradict the FO properties can be removed from the set. For instance, if a rejected observation exists within the convex hull of the accepted observations, which contradicts the convexity assumption of the FO model, it needs to be removed.

One future direction consists of focusing on special classes of convex problems and devising more efficient solution methods for large-case data-driven applications. Another area of future research is to consider the effect of data uncertainty on constraint inference and explore overfitting and robustness conditions for the inverse framework. We believe the method can also be applied in other application areas where an understanding of implicit expert constraints can help streamline the decision-making processes.

Appendix. Proofs

PROOF OF PROPOSITION 1. Constraints (2b)–(2c) ensure $\mathbf{x}^k \in \tilde{\mathcal{X}}, \forall k \in \mathcal{K}$, and constraints (2g)–(2i) use binary variables y_{ik} to ensure that at least one constraint (either inferred or known; linear or nonlinear) makes each rejected point infeasible, which, in turn, ensures $\mathbf{x}^k \notin \mathcal{X} \cap \tilde{\mathcal{X}}$. Therefore, the conditions of Definition 2 are met and $\tilde{\mathcal{X}}$ is a nominal set. Since the set $\tilde{\mathcal{X}} \cap \mathcal{X}$ is convex by definition, constraints (2b)–(2f) provide the necessary and sufficient KKT conditions to guarantee $\mathbf{x}^0 \in \arg \min_{\mathbf{x} \in \mathcal{X} \cap \tilde{\mathcal{X}}} \{f(\mathbf{x}; \mathbf{c})\}$. \square

PROOF OF PROPOSITION 2. To show that the feasible region is non-empty, we construct a solution (by assigning values to all variables $\mathbf{q}, \mathbf{a}, b, \lambda, \mu$, and y) that satisfies all constraints of DIO and is, hence, feasible. Let $\mathbf{q}_n = \hat{\mathbf{q}}, \forall n \in \tilde{\mathcal{N}}$, as defined in Assumption 1. By Assumption 3 and the Separating Hyperplane Theorem (Boyd and Vandenberghe 2004), for every rejected point $k \in \mathcal{K}^-, \exists \hat{\mathbf{a}}_k, \hat{b}_k$ such that $\hat{\mathbf{a}}'_k \mathbf{x}^k < \hat{b}_k$ and $\hat{\mathbf{a}}'_k \mathbf{x}^p \geq \hat{b}_k, \forall p \in \mathcal{K}^+$. Let $[\mathbf{a}_\ell] = [\hat{\mathbf{a}}_1, \dots, \hat{\mathbf{a}}_{|\mathcal{K}^-|}, \nabla f(\mathbf{x}^0; \mathbf{c}), \dots, \nabla f(\mathbf{x}^0; \mathbf{c})]$ and $\mathbf{b} = [\hat{b}_1, \dots, \hat{b}_{|\mathcal{K}^-|}, \nabla(\mathbf{x}^0; \mathbf{c})' \mathbf{x}^0, \dots, \nabla(\mathbf{x}^0; \mathbf{c})' \mathbf{x}^0], \quad \forall \ell \in \{1, \dots, \tilde{\mathcal{L}}\}$. Let the dual variables of the non-linear and linear constraints be $\lambda_n = 0, \forall n \in \mathcal{N} \cup \tilde{\mathcal{N}}$, and $[\mu_\ell] = [\mathbf{0}_{1 \times |\mathcal{L} \cup \tilde{\mathcal{L}}| - 1}, -1], \forall \ell \in \mathcal{L}$, respectively. Finally, let binary variables $y_{kk} = 0, \forall i \in \tilde{\mathcal{L}}, k \in \mathcal{K}^-$ and $y_{kk} = 1, \forall i \in \mathcal{I} \setminus \tilde{\mathcal{L}}, k \in \mathcal{K}^-$. By substitution, it can be seen that this constructed solution satisfies all constraints (2c)–(2m). Note that the first $|\mathcal{K}^-|$ constraints ensure that each rejected point is infeasible for at least one inferred linear constraint, and the last set of constraints (which are all identical) ensure the optimality of \mathbf{x}^0 . All constraints satisfy primal feasibility $\forall \mathbf{x}^k, k \in \mathcal{K}^+$. \square

PROOF OF PROPOSITION 3. Let $\mathcal{S} = \mathcal{X} \cap \tilde{\mathcal{X}}$ be an imputed set for FO. Assume that $\mathcal{S} \not\subseteq \mathcal{C}$. Then $\exists \hat{\mathbf{x}} \in \mathcal{S} \setminus \mathcal{C}$. We know that $\hat{\mathbf{x}} \notin \mathcal{V}$ since it contradicts the definition of the preferred solution \mathbf{x}^0 . Hence, $\hat{\mathbf{x}} \in \mathcal{V} \setminus \mathcal{C}$. Consider the following two cases:

Case 1: If $f(\mathbf{x}; \mathbf{c})$ is linear, then $\mathcal{C} = \mathcal{V}$ and $\mathcal{V} \setminus \mathcal{C} = \emptyset$, which is in contradiction with $\mathbf{x}^k \in \mathcal{V} \setminus \mathcal{C}$.

Case 2: If $f(\mathbf{x}; \mathbf{c})$ is nonlinear convex, then \mathcal{V} is non-convex, and hence $\mathcal{V} \setminus \mathcal{C}$ is non-convex. Given that \mathcal{C} is the tangent half-space of the sublevel set of $f(\mathbf{x}; \mathbf{c})$ at \mathbf{x}^0 , then \mathbf{x}^0 is on the boundary of \mathcal{V} . Because \mathcal{S} is convex, for any $\hat{\mathbf{x}} \in \mathcal{V} \setminus \mathcal{C}$, there must exist $\lambda > 0$ such that $\bar{\mathbf{x}} = \lambda \hat{\mathbf{x}} + (1 - \lambda) \mathbf{x}^0$ and $\bar{\mathbf{x}} \in \mathcal{S} \setminus \mathcal{V}$, which contradicts $\mathbf{x}^0 \in \arg \min_{\mathbf{x} \in \mathcal{S}} \{f(\mathbf{x}; \mathbf{c})\}$. \square

PROOF OF PROPOSITION 4. Both \mathcal{S} and \mathcal{C} are convex so $\mathcal{C} \cap \mathcal{S}$ is also convex. Because \mathcal{S} is a nominal set and \mathcal{C} includes all accepted observations, $\mathcal{C} \cap \mathcal{S}$ is also a convex nominal set. Finally, Since \mathcal{S} is a convex nominal set, it includes the convex hull of all observations, and $\mathbf{x}^0 \in \mathcal{S}$, and therefore, $\mathbf{x}^0 \in \mathcal{S} \cap \mathcal{C}$. Because \mathcal{C} is the tangent half-space to the sublevel set of $f(\mathbf{x}; \mathbf{c})$ at \mathbf{x}^0 , it is also given that $\mathbf{x}^0 \in \arg \min_{\mathbf{x} \in \mathcal{S} \cap \mathcal{C}} \{f(\mathbf{x}; \mathbf{c})\}$. Therefore, $\mathcal{S} \cap \mathcal{C}$ meets the criteria outlined in Definition 5 and is therefore an imputed feasible set.

PROOF OF THEOREM 1. (i) Any solution $\mathbf{a}, b, \mathbf{q}, \lambda, \mu, y$ of DIO is also a solution of RDIO because it has fewer constraints. (ii) Vice-versa, for any solution $\mathbf{a}, b, \mathbf{q}, y$ of RDIO there exists a solution of DIO since \mathcal{C} is appended to the known constraints and the stationarity and complementary slackness conditions can be re-written as:

$$\begin{aligned} \nabla f(\mathbf{x}^0; \mathbf{c}) + \sum_{n \in \mathcal{N} \cup \tilde{\mathcal{N}}} \lambda_n \nabla g_n(\mathbf{x}^0, \mathbf{q}_n) + \lambda_0 \nabla f(\mathbf{x}^0; \mathbf{c}) + \sum_{\ell \in \mathcal{L} \cup \tilde{\mathcal{L}}} \mu_\ell \mathbf{a}_\ell &= \mathbf{0} \\ \lambda_0 (f(\mathbf{x}^0; \mathbf{c}) - f(\mathbf{x}^0; \mathbf{c})) &= 0 \\ \lambda_n g_n(\mathbf{x}^0, \mathbf{q}_n) &= 0 \quad \forall n \in \mathcal{N} \cup \tilde{\mathcal{N}}, \\ \mu_\ell (b_\ell - \mathbf{a}'_\ell \mathbf{x}^0) &= 0, \quad \forall \ell \in \mathcal{L} \cup \tilde{\mathcal{L}} \\ \lambda_n, \mu_\ell &\leq 0, \quad \forall n \in \mathcal{N} \cup \tilde{\mathcal{N}}, \ell \in \mathcal{L} \cup \tilde{\mathcal{L}} \end{aligned}$$

All conditions are satisfied if we set $\lambda_0 = -1$ and $\lambda_n, \mu_\ell \leq 0, \forall n \in \mathcal{N} \cup \tilde{\mathcal{N}}, \ell \in \mathcal{L} \cup \tilde{\mathcal{L}}$. Hence, for any solution to RDIO, there exists a corresponding solution to DIO. Therefore, by (i) and (ii), the DIO and RDIO are equivalent when \mathcal{C} is added as a known constraint. \square

PROOF OF COROLLARY 1. Due to constraints (3b)–(3i), we know that $\tilde{\mathcal{X}}$ is a nominal feasible set for FO. Note that $\mathbf{x}^0 \in \mathcal{X} \cap \tilde{\mathcal{X}} \cap \mathcal{C}$ given that $\mathbf{x}^0 \in \mathcal{X}$ by Assumption 2, $\mathbf{x}^0 \in \tilde{\mathcal{X}}$ because $\tilde{\mathcal{X}}$ is a nominal set, and $\mathbf{x}^0 \in \mathcal{C}$ by definition. Furthermore, $\mathbf{x}^0 \in \mathcal{C} = \{\mathbf{x} \mid f(\mathbf{x}; \mathbf{c}) \geq f(\mathbf{x}^0; \mathbf{c})\}$, which implies that $\mathbf{x}^0 \in \arg \min_{x \in \mathcal{C} \cap \mathcal{X} \cap \tilde{\mathcal{X}}} f(\mathbf{x}; \mathbf{c})$ and is therefore an optimal solution of (4a). \square

References

Ahmadi F, Ganjkhaneh F, Ghobadi K (2020) Inverse learning: A data-driven framework to infer optimizations models. *arXiv preprint arXiv:2011.03038* .

Ahuja RK, Orlin JB (2001) Inverse optimization. *Operations Research* 49(5):771–783.

Ajayi T, Lee T, Schaefer AJ (2022) Objective selection for cancer treatment: an inverse optimization approach. *Operations Research* .

American Cancer Society (2022) Cancer Statistics Center. <http://cancerstatisticscenter.cancer.org> [Accessed: 18.06.2022].

Aswani A, Shen ZJ, Siddiq A (2018) Inverse optimization with noisy data. *Operations Research* 66(3):870–892.

Aswani A, Shen ZJM, A (2019) Data-driven incentive design in the medicare shared savings program. *Operations Research* 67(4):1002–1026.

Babier A, Boutilier JJ, Sharpe MB, McNiven AL, Chan TC (2018) Inverse optimization of objective function weights for treatment planning using clinical dose-volume histograms. *Physics in Medicine & Biology* 63(10):105004.

Babier A, Chan TC, Lee T, Mahmood R, Terekhov D (2021) An ensemble learning framework for model fitting and evaluation in inverse linear optimization. *Informs Journal on Optimization* 3(2):119–138.

Babier A, Mahmood R, McNiven AL, Diamant A, Chan TC (2020) Knowledge-based automated planning with three-dimensional generative adversarial networks. *Medical Physics* 47(2):297–306.

Bertsimas D, Gupta V, Paschalidis IC (2015) Data-driven estimation in equilibrium using inverse optimization. *Mathematical Programming* 153(2):595–633.

Birge JR, Hortaçsu A, Pavlin JM (2017) Inverse optimization for the recovery of market structure from market outcomes: An application to the MISO electricity market. *Operations Research* 65(4):837–855.

Boutilier JJ, Lee T, Craig T, Sharpe MB, Chan TC (2015) Models for predicting objective function weights in prostate cancer imrt. *Medical physics* 42(4):1586–1595.

Boyd S, Vandenberghe L (2004) *Convex optimization* (Cambridge university press).

Brucker P, Shakhlevich NV (2009) Inverse scheduling with maximum lateness objective. *Journal of Scheduling* 12(5):475–488.

Černý M, Hladík M (2016) Inverse optimization: towards the optimal parameter set of inverse LP with interval coefficients. *Central European Journal of Operations Research* 24(3):747–762.

Chan TC, Eberg M, Forster K, Holloway C, Ieraci L, Shalaby Y, Yousefi N (2022) An inverse optimization approach to measuring clinical pathway concordance. *Management Science* 68(3):1882–1903.

Chan TC, Kaw N (2020) Inverse optimization for the recovery of constraint parameters. *European Journal of Operational Research* 282(2):415–427.

Chan TC, Lee T (2018) Trade-off preservation in inverse multi-objective convex optimization. *European Journal of Operational Research* 270(1):25–39.

Chan TC, Lee T, Terekhov D (2019) Inverse optimization: Closed-form solutions, geometry, and goodness of fit. *Management Science* 65(3):1115–1135.

Chan TC, Mahmood R, Zhu IY (2021) Inverse optimization: Theory and applications. *arXiv preprint arXiv:2109.03920* .

Chan TC, Mahmoudzadeh H, Purdie TG (2014a) A robust-cvar optimization approach with application to breast cancer therapy. *European Journal of Operational Research* 238(3):876–885.

Chan TCY, Craig T, Lee T, Sharpe MB (2014b) Generalized inverse multi-objective optimization with application to cancer therapy. *Operations Research* 62(3):680–695.

Chow JYJ, Recker WW (2012) Inverse optimization with endogenous arrival time constraints to calibrate the household activity pattern problem. *Transportation Research Part B: Methodological* 46(3):463–479.

Dempe S, Lohse S (2006) Inverse linear programming. *Recent Advances in Optimization*, 19–28 (Springer).

Dong C, Zeng B (2018) Inferring parameters through inverse multiobjective optimization. *arXiv preprint arXiv:1808.00935* .

Esfahani PM, Shafeezadeh-Abadeh S, Hanasusanto GA, Kuhn D (2018) Data-driven inverse optimization with incomplete information. *Mathematical Programming* 167(1):191–234.

Gebken B, Peitz S (2021) Inverse multiobjective optimization: Inferring decision criteria from data. *Journal of Global Optimization* 80(1):3–29.

Ghate A (2020a) Imputing radiobiological parameters of the linear-quadratic dose-response model from a radiotherapy fractionation plan. *Physics in Medicine & Biology* 65(22):225009.

Ghate A (2020b) Inverse optimization in semi-infinite linear programs. *Operations Research Letters* 48(3):278–285.

Ghobadi K, Lee T, Mahmoudzadeh H, Terekhov D (2018) Robust inverse optimization. *Operations Research Letters* 46(3):339–344.

Ghobadi K, Mahmoudzadeh H (2021) Inferring linear feasible regions using inverse optimization. *European Journal of Operational Research* 290(3):829–843.

Goli A, Boutilier JJ, Craig T, Sharpe MB, Chan TC (2018) A small number of objective function weight vectors is sufficient for automated treatment planning in prostate cancer. *Physics in Medicine & Biology* 63(19):195004.

Güler Ç, Hamacher HW (2010) Capacity inverse minimum cost flow problem. *Journal of Combinatorial Optimization* 19(1):43–59.

Iyengar G, Kang W (2005) Inverse conic programming with applications. *Operations Research Letters* 33(3):319–330.

Keshavarz A, Wang Y, Boyd S (2011) Imputing a convex objective function. *2011 IEEE International Symposium on Intelligent Control (ISIC)*, 613–619 (IEEE).

Lee T, Hammad M, Chan TC, Craig T, Sharpe MB (2013) Predicting objective function weights from patient anatomy in prostate imrt treatment planning. *Medical physics* 40(12):121706.

Li JYM (2021) Inverse optimization of convex risk functions. *Management Science* 67(11):7113–7141.

Mahmoudzadeh H, Lee J, Chan TC, Purdie TG (2015) Robust optimization methods for cardiac sparing in tangential breast imrt. *Medical physics* 42(5):2212–2222.

Naghavi M, Foroughi AA, Zarepisheh M (2019) Inverse optimization for multi-objective linear programming. *Optimization Letters* 13(2):281–294.

Saez-Gallego J, Morales JM (2018) Short-term forecasting of price-responsive loads using inverse optimization. *IEEE Transactions on Smart Grid* 9(5):4805–4814.

Sayre G, Ruan D (2014) Automatic treatment planning with convex imputing. *Journal of Physics: Conference Series*, volume 489, 012058 (IOP Publishing).

Shahmoradi Z, Lee T (2021) Quantile inverse optimization: Improving stability in inverse linear programming. *Operations Research* .

Tavashioğlu O, Lee T, Valeva S, Schaefer AJ (2018) On the structure of the inverse-feasible region of a linear program. *Operations Research Letters* 46(1):147–152.

Troutt MD, Brandyberry AA, Sohn C, Tadisina SK (2008) Linear programming system identification: The general nonnegative parameters case. *European Journal of Operational Research* 185(1):63–75.

Troutt MD, Pang WK, Hou SH (2006) Behavioral estimation of mathematical programming objective function coefficients. *Management Science* 52(3):422–434.

Zhang J, Liu Z (1999) A further study on inverse linear programming problems. *Journal of Computational and Applied Mathematics* 106(2):345–359.

Zhang J, Xu C (2010) Inverse optimization for linearly constrained convex separable programming problems. *European Journal of Operational Research* 200(3):671–679.

Zhang J, Zhang L (2010) An augmented lagrangian method for a class of inverse quadratic programming problems. *Applied Mathematics and Optimization* 61(1):57–83.